

## SABRE observations of Pi2 pulsations: case studies

E. G. Bradshaw, M. Lester

Radio and Space Plasma Physics Group, Department of Physics and Astronomy, University of Leicester, Leicester, LE1 7RH

Received: 14 December 1994/Revised: 26 June 1996/Accepted: 22 July 1996

**Abstract.** The characteristics of substorm-associated Pi2 pulsations observed by the SABRE coherent radar system during three separate case studies are presented. The SABRE field of view is well positioned to observe the differences between the auroral zone pulsation signature and that observed at mid-latitudes. During the first case study the SABRE field of view is initially in the eastward electrojet, equatorward and to the west of the substorm-enhanced electrojet current. As the interval progresses, the western, upward field-aligned current of the substorm current wedge moves westward across the longitudes of the radar field of view. The westward motion of the wedge is apparent in the spatial and temporal signatures of the associated Pi2 pulsation spectra and polarisation sense. During the second case study, the complex field-aligned and ionospheric currents associated with the pulsation generation region move equatorward into the SABRE field of view and then poleward out of it again after the third pulsation in the series. The spectral content of the four pulsations during the interval indicate different auroral zone and mid-latitude signatures. The final case study is from a period of low magnetic activity when SABRE observes a Pi2 pulsation signature from regions equatorward of the enhanced substorm currents. There is an apparent mode change between the signature observed by SABRE in the ionosphere and that on the ground by magnetometers at latitudes slightly equatorward of the radar field of view. The observations are discussed in terms of published theories of the generation mechanisms for this type of pulsation. Different signatures are observed by SABRE depending on the level of magnetic activity and the position of the SABRE field of view relative to the pulsation generation region. A twin source model for Pi2 pulsation generation provides the clearest explanation of the signatures observed.

### 1 Introduction

Pi2 pulsations occur simultaneously with substorm expansion phase onset and subsequent intensifications. The primary generation of these waves, however, is believed to be on field lines that thread the auroral zone substorm break-up region. At substorm expansion phase onset, a section of the cross-tail current is diverted into the auroral ionosphere by the field-aligned currents (FAC) forming the substorm current wedge (McPherron *et al.*, 1973). This change in magnetosphere-ionosphere coupling is effected by the launching of Alfvén wave transients which redistribute this excess current (Southwood and Hughes, 1985), leading to the reconfiguration of the auroral zone geomagnetic field, the ionospheric electric field and auroral zone conductivities. This is observed in the ionosphere as the substorm enhanced westward electrojet. The transverse mode Alfvén wave is subsequently reflected from the conjugate ionosphere and bounces back and forth reducing in amplitude with each reflection due to ionospheric absorption. The Pi2 waveform at high-latitudes appears, however, broadband and ill-defined, unlike the mid-latitude signature which consists of damped, quasi-sinusoidal oscillations occurring at the start of a magnetic bay (Rostoker, 1967; Stuart, 1972). Although the mid-latitude Pi2 signature is well defined, there has been much debate on the generation mechanism. Southwood and Stuart (1980) have reviewed the observational evidence and the three proposals for this generation mechanism: a field line resonance, a surface wave on the plasmopause and a cavity mode resonance, all of which have been illustrated schematically by Yeoman and Orr (1989, their Fig. 1).

The substorm FAC, upward at the western edge of the wedge and downward at the eastern end, produce signatures in mid-latitude magnetometer records that enable identification of the position of the wedge with data from a longitudinal chain of magnetometer stations (Lester *et al.*, 1983; 1984). The H-component perturbation is

positive within the wedge and negative outside while the D-component perturbation is asymmetrical with respect to the wedge, being positive to the west of centre of the wedge and negative to the east of centre. The position where the D-component perturbation is zero marks the centre of the wedge.

Recently, the observation of Pi2 pulsations by the STARE radar has been reported (Sutcliffe and Nielsen, 1990, 1992). The derived pulsation electric field distributions contained regions of radial and linear electric field which were considered compatible with those produced by an Alfvén wave incident on a strip of enhanced ionospheric conductivity (Southwood and Hughes, 1985). However, these observed features did not persist throughout the whole Pi2 pulsation. Furthermore, Sutcliffe and Nielsen (1990, 1992) concluded that the most significant Pi2 signature observed by STARE in the ionospheric electron flow occurred poleward of the centre of the auroral break-up region. Pi2 pulsations have also been observed in data from the Wick component alone of the Sweden and Britain Radar-aurora Experiment (SABRE) coherent radar system (Nielsen *et al.*, 1983) in association with the SAMNET magnetometer array (Yeoman *et al.*, 1991). Yeoman *et al.* (1991) examined the polarisation, propagation and wave modes of Pi2 pulsations. These authors concluded that the sub-auroral latitudes are a transitional zone between the auroral zone Alfvén wave and mid-latitude compressional mode signatures of Pi2 pulsations. Hence, SABRE is ideally located to investigate the transition signatures of the pulsations.

In the present study, three substorm intervals containing Pi2 pulsations observed by SABRE are presented. A description of the experimental arrangement employed in this study is given elsewhere (Bradshaw *et al.*, 1994). Data from the British Geological Survey (BGS) magne-

ter array (Table 1) were employed to identify the Pi2 pulsations. In addition, data are also available for the three specific intervals of interest from the stations of the EISCAT magnetometer cross (Table 2) operated by the University of Braunschweig (Lühr *et al.*, 1984). A schematic map of northern Europe with the positions of the two magnetometer arrays relative to the SABRE field of view is presented in Fig. 1. The radar field of view covers the geographic range between 64° and 68°N and 0° and 12°E, equivalent to 60.5° to 66.9°N and 85.2° to 98.1°E geomagnetic.

The three substorm intervals were chosen from different levels of magnetic activity and at different local times to investigate the ionospheric Pi2 signatures at different positions relative to the substorm current wedge and the transition zone between auroral zone Alfvén and mid-latitude compressional pulsation signatures previously identified by Yeoman *et al.* (1991). The SABRE field of view can be located at the perfect latitude to observe the different time series, spatial and spectral signatures of the Pi2 pulsations in the auroral zone and those at mid-latitudes. The purpose of this study is to demonstrate the complexity of the electric field signatures associated with the Pi2 pulsations in this transition zone.

## 2 Case interval 1: eastward electrojet Pi2 pulsations

### 2.1 SABRE and magnetometer pulsation signatures

The first case study to be considered consists of two Pi2 pulsations, at 17:36 UT and 17:48 UT (Fig. 2). The H-component (north-south) measured at Nordli (NI), the Faroes (FA) and Wick (WI) (Fig. 2a, top three panels) indicates a positive bay at Nordli for both events but only

**Table 1.**

BGS Magnetometer Station	Geographic latitude (°N)	Geographic longitude (°E)	Geomagnetic latitude (°N)	Geomagnetic longitude (°E)
Tromsø (TR)	69.6	19.0	66.4	104.2
Nordli (NI)	64.5	13.5	61.6	96.1
Faroes (FA)	62.0	− 7.0	61.3	78.9
Lerwick (LE)	60.1	− 1.2	58.5	82.2
Wick (WI)	58.4	− 3.1	56.9	79.8

**Table 2.**

EISCAT cross Magnetometer station	Geographic latitude (°N)	Geographic longitude (°E)	Geomagnetic latitude (°N)	Geomagnetic longitude (°E)
Sørøya (SOR)	70.5	22.2	67.3	107.9
Alta (ALT)	69.9	23.0	66.6	107.8
Kautokeino (KAU)	69.0	23.1	65.8	107.2
Muonio (MUO)	68.0	23.5	64.7	106.7
Pello (PEL)	66.9	24.1	63.6	106.0
Sodankylä (SOD)	67.4	26.6	63.6	108.5
Kilpisjärvi (KIL)	69.1	20.7	66.0	105.5
Kevo (KEV)	69.8	27.0	66.2	110.6

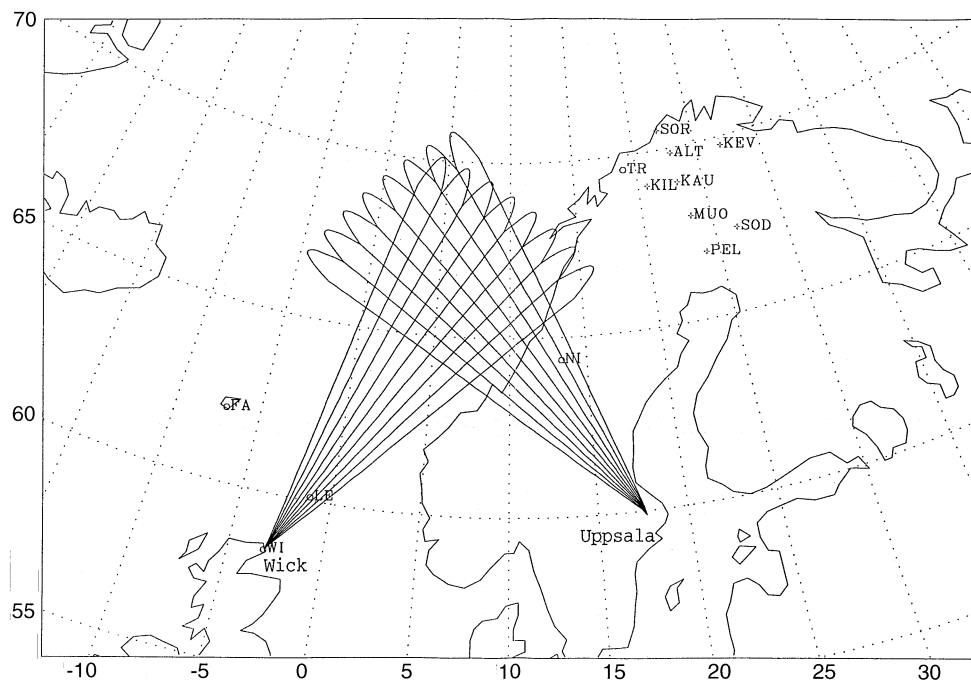


**Fig. 1.** A schematic diagram to illustrate the location in geographic latitude and longitude of the SABRE field of view, the position of the BGS magnetometers ( $\odot$ ) and the stations of the EISCAT magnetometer cross (+)

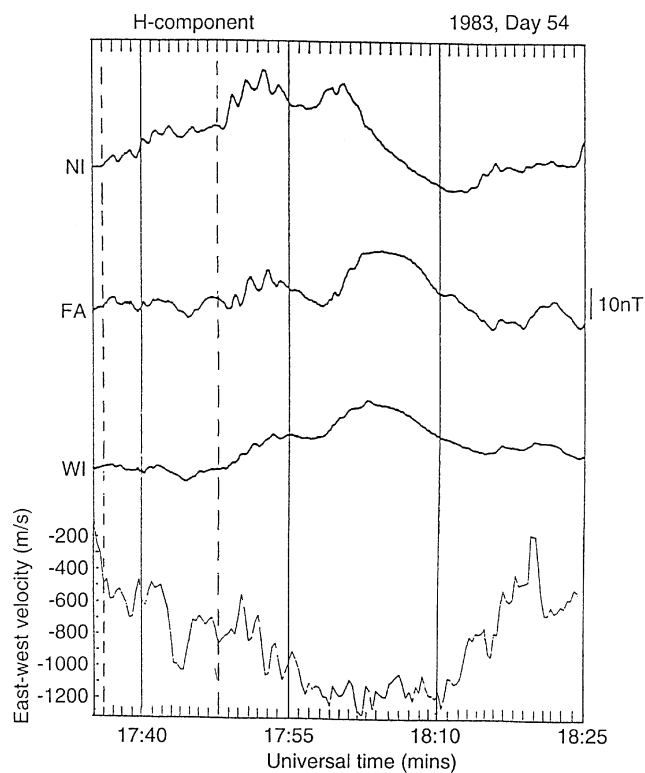
for the second event at the Faroes and Wick. The D-components (east-west) for the same three magnetometer stations (Fig. 2b, top three panels) indicate positive bays at all three stations for the first event but weakly negative at Nordli for the second. In each case the overall change in field magnitude is calculated as the difference between the component value after the pulsation and that at onset (Lester *et al.*, 1983). Identification of the location of the FAC of the substorm current wedge from mid-latitude magnetograms can lead to an overestimation of the width of the current wedge (Lester *et al.*, 1989; Sergeev *et al.*, 1996). Thus, the upward FAC for event 1 is placed to the east of the Faroes, whilst for the second event it is placed at or near the Faroes. The centre of the wedge on the other hand is well determined from mid-latitude magnetograms (Lester *et al.*, 1989), and moves from east of Nordli for event 1 to west of Nordli for event 2, although the D component bay at Nordli for the second event is only weakly negative.

The EISCAT magnetometer cross data, although up to an hour east of SABRE, can provide useful information on the electrojet currents when the pulsations occur. At 17:30 UT, in the EISCAT cross magnetometer data (not shown), there is a negative X-component (north-south) bay at ALT and positive X-component bays at KAU, MUO, PEL and SOD. At these latter stations these bays become negative at  $\sim 17:43$  UT. The Z-component bays are negative at ALT, KAU and MUO at 17:30 UT, whilst at PEL and SOD they are initially weakly positive and then negative at  $\sim 17:43$  UT. These data indicate that initially a westward electrojet is centred poleward of ALT and an eastward electrojet is centred near SOD. The westward electrojet eventually dominates the whole

array following 17:43 UT, but is still centred poleward of ALT.

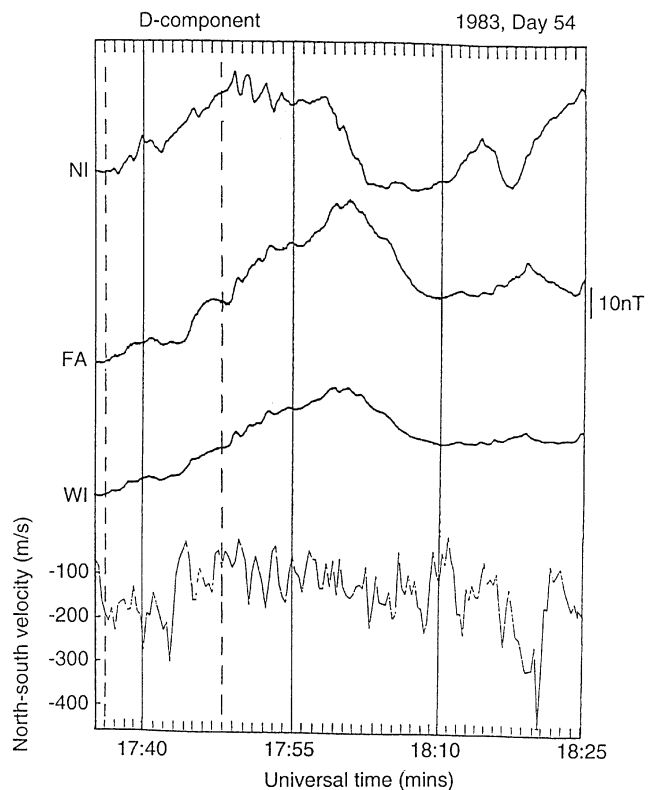
The westward component of the drift velocity measured by SABRE in the prescribed latitude and longitude cell during both intervals (Fig. 2a, bottom panel) implies this part of the radar field of view is in the eastward electrojet at the time of these pulsations. Furthermore, the irregularity drift velocity increases in magnitude in the westward direction following the second event, indicating an enhancement of the eastward electrojet at the latitude illustrated in Fig. 2a and the local time of SABRE. Spatial plots of the velocity (Fig. 3) illustrate that, throughout the first pulsation, the background ionospheric velocity was mostly westward as would be expected for a background eastward electrojet. The magnitude of the velocity in the equatorward part of the field of view, below  $65.0^\circ\text{N}$ , is stronger than the velocity poleward of  $65.0^\circ\text{N}$ , indicative of a boundary between the two regions of flow. The magnetometer records from Nordli and Faroer suggest that the SABRE field of view is at longitudes which encompass the substorm current wedge. It is concluded, therefore, that for both the Pi2 pulsations the enhanced westward electrojet associated with the substorm current wedge is located poleward of the SABRE field of view during this interval. This is consistent with the EISCAT cross data for the first Pi2 event.

There is some evidence in both the ground magnetometer and SABRE east-west velocity component data of further Pi2 pulsation activity between 17:58 UT and 18:04 UT and from 18:16 UT to 18:20 UT (Fig. 2a). These pulsations did not form a detailed part of this investigation, however, as they occurred when the SABRE field of view was observing characteristic signatures of



Start time: 1983 54 17 35 0  
64.6-64.8°North, 6.0-8.0°East

a



Start time: 1983 54 17 35 0  
64.6-64.8°North, 6.0-8.0°East

b

ionospheric flow associated with the WTS (Bradshaw *et al.*, 1994).

### 2.2 Spectral analysis

Maximum entropy (ME) spectral analysis of the two pulsations under investigation was performed and the dominant wave periods are given in Table 3. The dominant period in the SABRE east-west velocity component and the ground magnetometer records compare favourably although in some cases no spectral peaks were identified in the Pi2 pulsation band in the magnetometer data. It is noted, however, that there is a non-trivial uncertainty involved in measuring the peaks of the maximum entropy spectra. Such uncertainty may account for instances where the dominant periods in magnetometer and radar data differ slightly but large differences observed by the radar and ground magnetometers are most likely to be due to a geophysical reason.

The spatial variation of the wave spectral power at the dominant pulsation period over the full SABRE field of view is summarised in Table 4 for the two separate velocity components. During the first pulsation the wave power in the east-west component is strongly localised to an elliptical region in the south-eastern part of the field of view below 65°N. At the time of the second pulsation, the area of peak power in the east-west component expanded in longitude but contracted in latitude, and moved westwards while remaining centred at the same latitude. The wave spectral power in the north-south component is of lesser strength and, for the first event, is centred around a single cell, 65.6–65.8°N, 7.5–8.0°E. For the second event, however, the wave spectral power exhibits a double structure, both of which are equatorward of the peak power in the first event. The wave spectral power at the dominant frequency for the second pulsation is localised in the high velocity region mentioned earlier.

### 2.3 Polarisation analysis

Polarisation hodograms for the two pulsations were constructed from the raw east-west and north-south velocity components in the regions of the SABRE field of view where the wave spectral power at the dominant pulsation period was high. This is equivalent to examining the two orthogonal components of the ionospheric electric field associated with the Pi2 pulsation. As the velocity is merely rotated 90° clockwise and scaled according to 1000 m s<sup>-1</sup>, equivalent to an electric field of 50 mV m<sup>-1</sup>, the polarisation sense of the hodograms is unaffected by

←  
**Fig. 2.** a Unfiltered ground magnetometer H-component data from Nordli, Faroes and Wick compared with SABRE east-west velocity component data (positive east) averaged over a small region of the field of view, 64.6° to 64.8°N and 6° to 8°E. Dashed lines delineate the onset times of the two Pi2 pulsations at 17:36 UT and 17:49 UT; b the same time series data as a but for ground magnetometer D-component data compared with the SABRE north-south velocity component data (positive north).

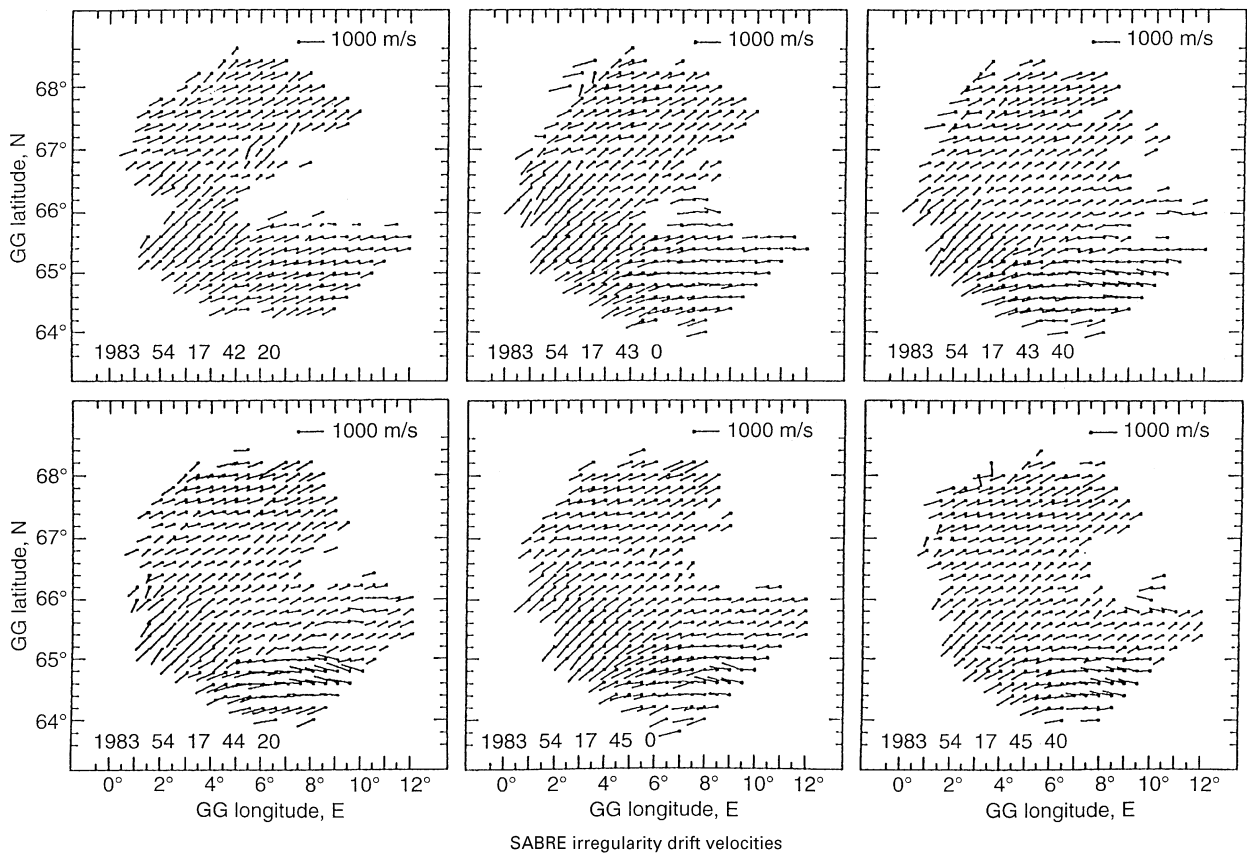


**Fig. 3.** A sequence of SABRE spatial velocity plots starting just at the end of the first pulsation (17:42:20 UT) and in the interval between the two pulsations. The region of enhanced velocity appears

about 17:43 UT toward the equatorward edge of the field of view and remains until after the end of the second pulsation

**Table 3.**

	Period (s)	
	ME	
Pi2 Pulsation: 17:36–17:42 UT		
Magnetometer	H	D
Faroes (FA)	111	No peak
Nordli (NI)	111	111
Wick (WI)	No peak	No peak
SABRE	107	
Pi2 Pulsation: 17:48–17:55 UT		
Magnetometer	H	D
Faroes (FA)	91	91
Nordli (NI)	91	100
Wick (WI)	100	100
SABRE	95	

this transformation. For the first pulsation, at 17:36 UT, two regions of different polarisation are found, anti-clockwise (ACW) in the west and clockwise (CW) in the east. In addition to the longitudinal separation, with the boundary at around  $4.5^\circ\text{E}$ , there is also a latitudinal demarcation between the two regions at around  $65.6^\circ\text{N}$ . The

polarisation sense in these two regions remains the same throughout the first pulsation. Outside these two regions the wave spectral power at the dominant pulsation period is low and it is not meaningful to construct polarisation hodograms. Throughout the second pulsation, at 17:48 UT, the polarisation sense is everywhere CW at positions in the SABRE field of view exhibiting high wave spectral power at the dominant pulsation period. There is no change in the polarisation sense during the second pulsation.

#### 2.4 Summary of case study 1

During this first case study, the westward velocities (eastward electrojet) observed in the SABRE field of view, taken in conjunction with the EISCAT-X magnetometer data, indicate that the SABRE field of view is located equatorward of the substorm-enhanced westward electrojet. The Nordli and Faroer magnetometer data position the field of view at longitudes which encompass the substorm current wedge. In particular, the upward FAC at the western end of the wedge and the wedge centre are demonstrated to have moved westwards across the longitudes of the SABRE field of view between the two pulsations. The spectral and spatial characteristics of the two

**Table 4.**

	Event 1	Event 2
Spectral power east-west component	64.6–65.0°N 8.5–10.0°E	64.6–64.8°N 6.0–9.0°E
north-south component	65.6–65.8°N 7.5–8.0°E	64.2–65.0°N, 65.4–65.6°N 6.0–8.0°E 3.0–5.0°E
Spatial velocity	Mostly uniform Westward	Enhanced flow 64.2–65.0°N
Velocity magnitude	Uniform	Shear ~65.0°N
Polarisation	2 regions ACW > 65.6°N, < 5.0°E CW < 65.6°N, > 4.0°E	CW everywhere

Pi2 pulsations observed within the SABRE field of view during the first substorm interval are summarised in Table 4. These changing pulsation characteristics are observed at latitudes equatorward of the substorm enhanced westward electrojet, and therefore the auroral break-up, but within the longitude range of the substorm current wedge. When examining the spatial velocity patterns at substorm onset it has been observed that, in the majority of cases, the background velocity is westward rather than the expected eastward velocity associated with the substorm enhanced westward electrojet when the magnetometer data position the radar field of view within the substorm current wedge (Yeoman *et al.*, 1991; Bradshaw *et al.*, 1994). These authors suggested that the wedge may have a more complicated velocity structure than just an enhanced eastward velocity. In this case study there was a pronounced enhancement in westward velocity during the second event which is spatially identified with the region of peak wave spectral power at the dominant pulsation frequency.

Further evidence for the westward movement of the onset region may be obtained by considering the four-quadrant, multi-region polarisation pattern derived from magnetometer data ordered by the substorm centred coordinates (Pashin *et al.*, 1982; Samson and Harrold, 1983; Samson and Rostoker, 1983). Based upon this model, the change from ACW to CW polarisation sense when going from higher to lower latitudes observed by SABRE places the radar field of view at the western edge of the substorm onset region for the first pulsation. The CW polarisation for the second pulsation would place the SABRE field of view even closer in longitude to the centre of the onset region but still below the onset latitude, implying a westward movement of this region from event 1 to event 2. This is consistent with the substorm current wedge locations determined earlier. The model of Pashin *et al.* (1982) predicts an enlargement and westward movement of this region of enhanced current. The region of peak wave spectral power at the dominant pulsation period observed by SABRE also moves to the west and enlarges in longitudinal extent between the two pulsations. The complete polarisation pattern is not observed in this study because the regions of peak wave spectral power are relatively small and the width of the field of view ( $12^\circ$ ) is too small to observe the total current system, typically  $40^\circ$  of longitude (Samson and Harrold, 1983).

Field-line resonance theory predicts an amplitude maximum and a latitudinal change in polarisation sense about the latitude of the resonance region (Southwood, 1974; Chen and Hasegawa, 1974). Such a latitudinal reversal in Pi2 polarisation sense has been observed previously in ground magnetometer data (Björnsson *et al.*, 1971; Fukunishi, 1975). A latitudinal change in polarisation sense is only observed for the first pulsation. There are no FFT derived amplitude and phase measurements across the SABRE field of view available for this interval because of the short period and duration of the pulsations. Thus, it is not possible to state definitively that either or both of the pulsations arise from a field line resonance mechanism.

Yeoman *et al.* (1990) propose a twin source Pi2 pulsation generation model which has two main regions of different polarisation sense. The two areas of differing polarisation in event 1 have the opposite sense to those suggested by Yeoman *et al.* (1990) in their twin source Pi2 pulsation generation model. There is only a single region of CW polarisation in the SABRE field of view for the second pulsation. In the Yeoman *et al.* (1990) model such a polarisation sense implies the radar was in the region dominated by the auroral zone source.

In summary, the pulsations in this case study are best described by models featuring the interaction of field-aligned and ionospheric currents with the SABRE field of view situated equatorward and to the west of the region of onset initially but becoming closer for the second pulsation.

### 3 Case interval 2: SABRE auroral zone signatures associated with Pi2 pulsations

#### 3.1 SABRE and magnetometer signatures

During the interval 23:30 UT on day 355, 1982 to 00:20 UT on day 356, 1982 four Pi2 pulsations occurred, all of which are well resolved by SABRE (Fig. 4). Magnetometer data are only available from the mid-latitude BGS station at Wick and from the stations of the EISCAT cross for this interval. The Wick magnetogram indicates pulsations at 23:40 UT, 23:49 UT, 23:54 UT and 00:14 UT. The unfiltered magnetogram from Wick at the time of the first three pulsations displays features which are similar to

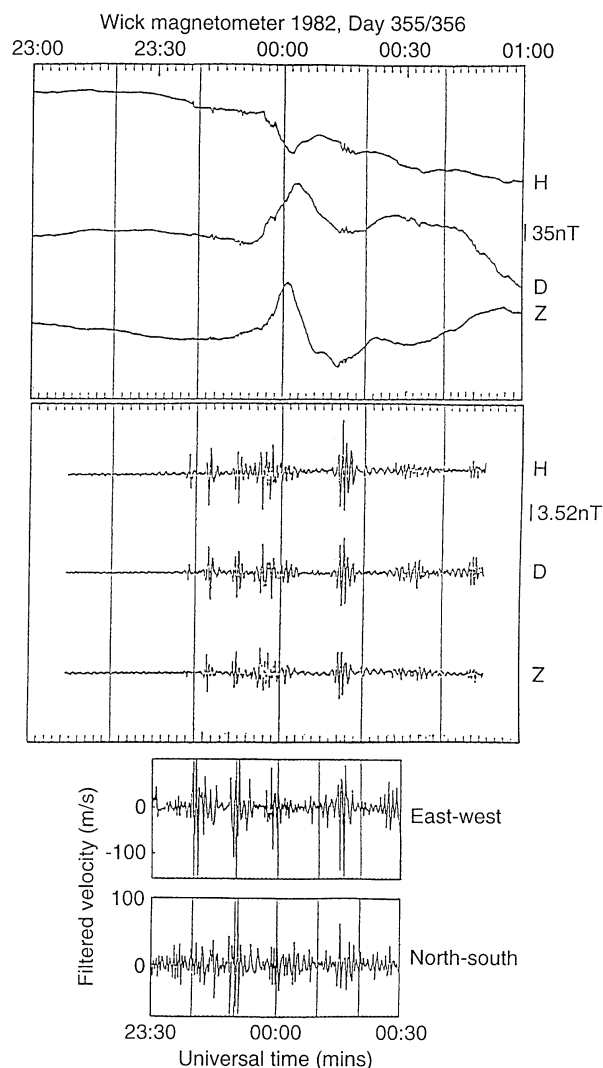


**Fig. 4.** Time series data for the event on day 355/356 1982. From *top to bottom* of the figure, unfiltered and filtered ground magnetometer data from the only operational BGS station at this time (Wick) are presented together with filtered SABRE east-west and north-south velocity component data

those caused by the passage overhead or slightly poleward of a WTS (Kisabeth and Rostoker, 1973). There is a sharp decrease in the already negative H-component, a pronounced positive onset in the D-component and an initial positive Z-component bay which turns negative at 00:02 UT. This interval is very disturbed in the EISCAT cross data and the magnetometer data are difficult to interpret. The main feature is a clear negative X-component bay at 00:00 UT which is largest at MUO and SOD indicating that the westward electrojet is centred close to these stations. The EISCAT magnetometer cross Z-component data indicate that all available stations are situated to the north of centre of the westward electrojet during the first three pulsations. As the lowest latitude station SOD is at  $67.4^{\circ}\text{N}$  geographic, the centre of the westward electrojet must be equatorward of this and, therefore, at a similar latitude to the centre of the SABRE field of view.

**Table 5.**

Event	Wick magnetometer		SABRE
	H-component period (s)	D-component period (s)	East-west velocity Component period (s)
Pi2 23:40–23:44	77	77	93 ( $65.4^{\circ}\text{N}$ , $7.5^{\circ}\text{E}$ )
Pi2 23:48–23:52	53	63	87 ( $66.6^{\circ}\text{N}$ , $2.0^{\circ}\text{E}$ )
Pi2 23:54–23:59	91	100	127 ( $65.0^{\circ}\text{N}$ , $4.5^{\circ}\text{E}$ )
Pi2 00:14–00:19	67	67	138 ( $68.0^{\circ}\text{N}$ , $4.0^{\circ}\text{E}$ ) 62 ( $65.2^{\circ}\text{N}$ , $6.0^{\circ}\text{E}$ )

### 3.2 Spectral analysis

The results of a comparative ME spectral analysis of the Wick magnetometer and SABRE data are given in Table 5. The majority of the wave spectral power is found in the east-west velocity component of the SABRE data. The dominant period at Wick is considerably lower than that in the SABRE data for all four pulsations. The spectrum at SABRE of the last pulsation does have a secondary peak (62 s) with only slightly less spectral power than the dominant period which is close to the dominant period at Wick (67 s). The differences in pulsation period may result from the complex system of FAC and ionospheric currents present at the time of the pulsation (see later) which suggest that the SABRE field of view is located close to the generation region of the pulsations whereas Wick is equatorward and observes the single resonant pulsation period normally seen at lower latitudes.

The spatial distribution of the wave spectral power at the dominant pulsation period was also investigated for each of the four Pi2 pulsations during this interval. In each case the peak wave spectral power is concentrated in a single cell in the SABRE field of view (Table 5). In the case of the fourth pulsation there are two regions of peak wave spectral power apparent, corresponding to the two pulsation periods present. There is no consistent motion of the position of the peak wave spectral power from event to event. In five of twenty-two intervals of multiple pulsation onsets, Bradshaw (1989) observed that the position in the SABRE field of view of the cell exhibiting peak wave spectral power oscillates to the east and west in an apparently random manner. Similar observations were presented by Gelpi *et al.* (1985) in a study of eleven substorm intervals at mid-latitudes. Due to the highly localised regions of spectral power it has not been possible to conduct a polarisation analysis over even a limited part of the radar field of view.

### 3.3 SABRE spatial velocity patterns

The SABRE spatial velocity patterns observed during this sequence of Pi2 pulsations are typical of those observed at and following substorm-expansion phase onset (Bradshaw *et al.*, 1994). The background velocity is initially eastward throughout the field of view but at the

onset of the first Pi2 pulsation at 23:40 UT, a region of south-eastward velocity appears in the north-east of the field of view and moves equatorward through the field of view until only this band of north-west to south-east oriented south-eastward velocity is in the field of view. This pattern remains until 23:49 UT, just after the onset of the second Pi2, when the velocity turns sharply equatorward for 40 seconds (Bradshaw *et al.*, 1994, Fig. 5) before returning to a south-eastward direction for a minute. Towards the end of the second pulsation at 23:50:40 UT, however, a different, more complex, feature is observed in the spatial velocity pattern. The poleward half of the region of south-eastward velocity rotates to point strongly eastward while the equatorward half remains as it was (Fig. 5). These two regions then move apart slightly as time progresses. The gaps between the different regions and a shear in the ionospheric spatial velocity pattern suggest the presence of FAC sheets (Waldock *et al.*, 1988), the enhanced conductivity having shorted-out the ionospheric electric field.

The electric field distribution associated with the substorm ionospheric and FAC at  $\sim 23:51$  UT (Fig. 5) during the time of the second pulsation can be obtained by rotating the velocity vectors clockwise through  $90^\circ$ . In the westward electrojet (eastward velocities) the electric field is directed toward the gap in the spatial velocity patterns

from the poleward side and away from the gap on the equatorward side. This implies that an upward FAC sheet is located poleward of a downward FAC sheet in agreement with the distribution of substorm FAC modelled by Baumjohann *et al.* (1981) at the time of a local auroral break-up.

These electric field structures are similar to those proposed by Southwood and Hughes (1983, Fig. 9) to give rise to a spatially localized transverse magnetic perturbation on the ground. In their simplest case a pair of upward and downward FAC are closed by Pedersen currents in the ionosphere. Southwood and Hughes (1983, Fig. 12) also present a similar pair of FAC and ionospheric electric field configuration resulting from a change in ionospheric conductivity and the launching of an Alfvén wave impulse at substorm onset. The SABRE electric field vectors, however, are not parallel on either side of the gap as suggested by the simple schematic of Southwood and Hughes (1983) but this could be caused by a non-uniform conductivity distribution in the ionosphere.

A final possible explanation is that the observed electric field configuration may represent that suggested by Southwood and Hughes (1985) in their travelling wave model for Pi2 pulsations. However, the 'highly conducting strip' envisaged in this model would have to be very narrow to explain the observations presented here.

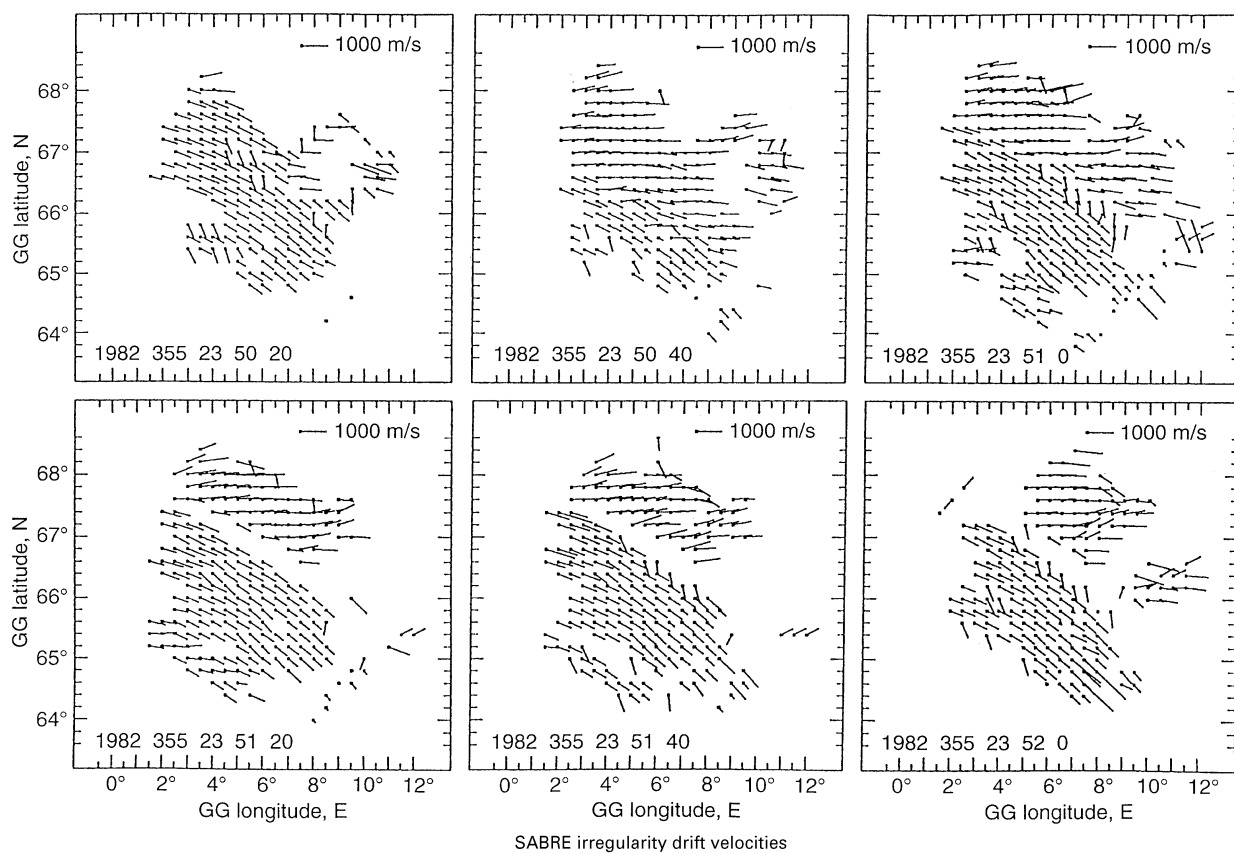


**Fig. 5.** A sequence of 20 s resolution SABRE spatial velocity plots from day 355, 1982 at the time of the second Pi2 pulsation where a region of strongly eastward velocity replaces the south-eastward

velocity that had been present. The two separate regions then move apart, the shear and gap between the two perhaps indicating the presence of a sheet of field-aligned current



Conversely however, Bradshaw (1989) found that the wave spectral power at the dominant Pi2 pulsation period in the SABRE data was normally very localised to only one or two cells in the SABRE field of view. In this case the cells are not coincident with the highly conducting strip (Fig. 5 and Table 5).

A similar highly structured velocity pattern was present at the onset time of the third pulsation (23:54 UT). The two distinct regions of velocity above have each rotated ACW by  $\sim 45^\circ$ . The equatorward region of south-eastward velocity is now eastward directed while the poleward region of eastward velocity is now north and north-eastward directed. The changed orientation of the two separate regions of velocity between the second and third Pi2 pulsations may have arisen from changes in the non-uniform ionospheric conductivity distribution and/or electric fields. This configuration remains until 23:55 UT at which time the two regions of velocity move poleward out of the field of view to be replaced by purely eastward velocity throughout the field of view by 23:56 UT.

At the onset of the final Pi2 pulsation in the series, 00:14 UT, a region of poleward velocity is observed in the north-west of the SABRE field of view, accompanied by the disappearance of a large region of backscatter from the east of the field of view. This situation lasts until the end of the pulsation at 00:19 UT, the velocity then returning to the steady eastward velocity typical of the westward electrojet. The peak in the wave spectral power at the longer of the two pulsation period components observed by SABRE during this interval was centred on this region of poleward velocity.

### 3.4 Summary of case interval 2

The SABRE spatial velocity data observed during this case study indicate the complex system of field-aligned and ionospheric currents during the magnetospheric substorm, and the manner in which these currents change as the substorm progresses. At the onset of the first pulsation, a region of south-eastward velocity moves equatorward through the field of view to fill it until the onset of the second pulsation. At this time the velocity turns sharply equatorward for 40 s before returning to a south-eastward direction. Subsequently, before the end of the second pulsation, the velocity splits into two distinct regions indicating the appearance in the ionosphere of a pair of FAC. This pattern evolves further at the time of the third pulsation with both regions rotating ACW by a similar amount to produce a new configuration of ionospheric and FAC. Towards the end of the pulsation, both regions move poleward out of the field of view leaving purely eastward velocity typical of the westward electrojet. A region of poleward velocity appears in the north-west of the field of view for the duration of the final pulsation before the velocity returns to eastward throughout the field of view once more.

The most interesting feature of the Pi2 pulsations observed by SABRE during this case study is the difference in dominant pulsation periods observed by SABRE and the Wick magnetometer. For the first three pulsations, the

SABRE period is always longer. The field-line resonance mechanism would produce a longer period at higher latitudes from a broadband, transient magnetospheric source associated with an earthward surge of plasma at substorm onset coupling to the geomagnetic field. Alternatively, the two different periods may result from two separate sources, one a transient Alfvénic source at high-latitudes, the other from a monochromatic, lower latitude cavity resonance source (Yeoman *et al.*, 1990). If this is the case, then the SABRE field of view is in the region of influence of both the transient, high-latitude auroral zone source and the lower latitude cavity resonance source at the time of the final of the four pulsations. The separation in longitude as well as in latitude of the two spectral peaks in the SABRE field of view implies an additional longitudinal separation of the two sources as described in the model (Yeoman *et al.*, 1990).

## 4 Case interval 3: low magnetic activity signature of SABRE Pi2 pulsations

### 4.1 Introduction

Four Pi2 pulsations occurred in the interval 20:40 UT to 21:20 UT on day 101, 1983 (Fig. 6). The Nordli magnetogram indicates pulsations at 20:48 UT, 20:54 UT, 21:05 UT and 21:11 UT. Magnetic activity was low at this time ( $K_p = 2-$ ,  $Lerwick-K = 1$ ). The EISCAT cross magnetometer data (not shown) indicate weak ( $\sim 50$  nT) negative X-component bays at ALT, KAU and MUO starting at 20:47 UT and lasting until 20:55 UT at which time they become positive. At ALT, the Z-component increases by  $\sim 50$  nT between 20:47 and 20:57 UT before decreasing. At KAU, the Z-component decreases initially at 20:47 UT before increasing from 20:50 to 21:00 UT and then decreasing again. The size of the bays suggest weak substorm electrojets at the time of the first two pulsations and indicate a westward electrojet at 20:47 UT centred between KAU and ALT, which changes to an eastward electrojet at  $\sim 20:57$  UT. Furthermore, there is no significant X-component bay activity at either PEL or SOD. If extended westwards, this eastward electrojet would be at a similar geomagnetic latitude to the location of the poleward, continuous velocity region observed within the SABRE field of view which is therefore located equatorward of the auroral zone generation region for the Pi2 pulsations during this interval.

Backscatter returns are first observed by SABRE during this interval at the onset of the first pulsation at 20:49 UT and die-out at 21:05 UT (Fig. 6) indicating that the backscatter appears to have been produced by the onset of the first pulsation. There is a small amount of backscatter during the last event. Backscatter does not fill the complete field of view during these two events but is limited to a region between  $66.0^\circ\text{N}$  and  $68.0^\circ\text{N}$  and can be divided into two regimes. Poleward of  $67.0^\circ\text{N}$  a region of backscatter is present throughout the two events. This region moves slowly equatorward during the interval but remains separate from the second, smaller backscatter region which is equatorward of  $67.0^\circ\text{N}$  and appears and

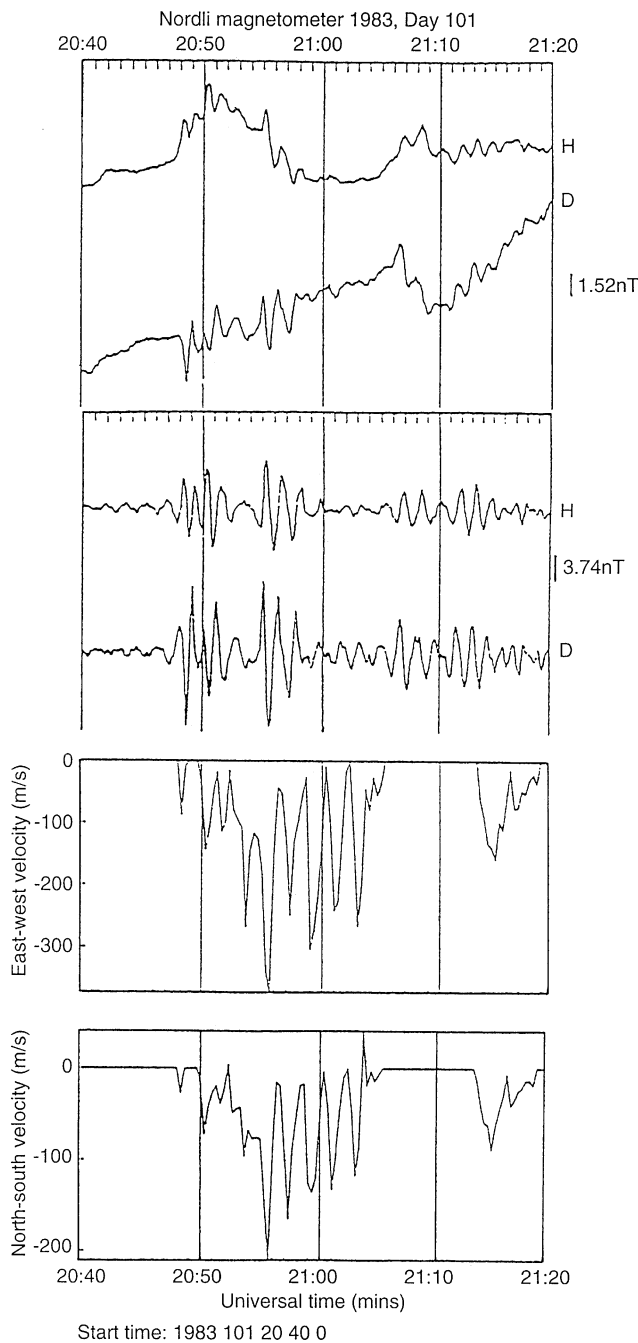


**Fig. 6.** Time series data for the Pi2 pulsations present on day 101, 1983. From *top to bottom*, unfiltered and filtered ground magnetometer data from Nordli are presented together with SABRE east-west and north-south velocity component data. The SABRE data were averaged over the small region of backscatter present during the event, from  $66^\circ$  to  $67.6^\circ\text{N}$  and  $4^\circ$  at  $6^\circ\text{E}$

disappears during the interval. The SABRE east-west and north-south velocity component time series data presented in Fig. 6 were obtained by averaging over all the backscatter present, i.e. between  $66^\circ$  and  $67.6^\circ\text{N}$  and  $4^\circ$  to  $6^\circ\text{E}$ . Ground magnetometers average over an area of scale size 100 km in the ionosphere so that features of smaller scale size are averaged out of ground magnetometer data (Hughes, 1974). The smaller equatorward

region of backscatter observed by SABRE during this period has a scale size of this order or less, which may account for some of the differences in the signatures observed.

#### 4.2 SABRE and magnetometer pulsation signatures

The SABRE time series of the two irregularity drift velocity components differ from those observed by the BGS ground magnetometer at Nordli (Fig. 6). Although the onset of backscatter returns observed by SABRE is coincident with the first pulsation on the ground, SABRE does not observe this pulsation well. The first clear oscillations in the SABRE data appear before the onset of the second pulsation on the ground and continue after the end of the second pulsation in the magnetometer data. The construction of a time series by averaging over the whole region of backscatter observed during the pulsation (Fig. 6, bottom) indicates that the poleward backscatter region produces a bay-like signature on top of which the equatorward on-off backscatter returns superimpose the oscillatory signature of the pulsation. The radar data from the ionosphere suggest a sequence of two pulsations, the first is of low amplitude, of similar period to, and coincident with, that observed on the ground. There is then a simultaneous phase skip in both data sets at about 20:53:40 UT between the two pulsations indicating the arrival or commencement of the second wave packet simultaneously at both the radar and magnetometer sites. The second pulsation however has different characteristics in the ground magnetometer and radar data as discussed later.

#### 4.3 Spectral analysis

Visual inspection of the respective waveforms indicates that the pulsation periods observed on the ground and in the ionosphere are somewhat different. On the ground, the dominant ME period for the first pulsation is about 60 s and this increases to around 90 s for the second. SABRE does not observe the first pulsation well but the pulsation period appears similar to that on the ground. The dominant ME period for the five cycles of the SABRE pulsation starting just before 20:54 UT is 117 s.

As this pulsation has a longer period in the SABRE data than those considered in the previous intervals and is observed for five cycles, it was also possible to undertake FFT spectral analysis on the SABRE data obtained for this pulsation. The dominant period occurs at 113 s, in agreement with the ME spectral analysis within the resolution of the SABRE FFT spectrum. The amplitude and phase characteristics of the SABRE east-west velocity component at this dominant period are presented in Fig. 7. The phase variation as a function of latitude is very complicated around the position of the amplitude peak. The longitudinal phase difference of  $\sim 50^\circ$  in  $\sim 3^\circ$  of longitude implies an azimuthal wave number ( $m$  value) of  $\sim 17$  and the phase leading in the east indicates a westward propagating wave. The majority of Pi2 pulsations observed normally display westward phase motion although

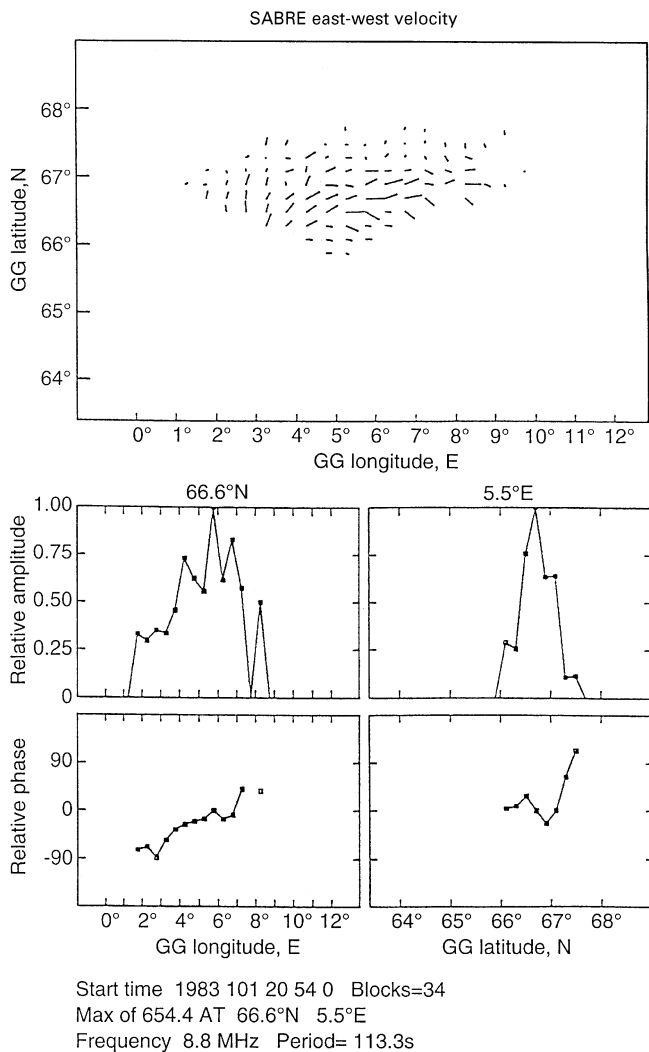


**Fig. 7.** Amplitude and phase characteristics throughout the SABRE field of view (*top*) determined from FFT spectral analysis of the SABRE east-west velocity component data on day 101, 1983. The amplitude (*middle*) and phase (*bottom*) as a function of latitude are very complicated around the amplitude peak while the longitudinal phase difference of  $\sim 50^\circ$  in  $\sim 3^\circ$  of longitude implies an  $m$  value of  $\sim 17$  and a westward propagating wave

the  $m$ -value is normally a lot smaller, typically  $< 4$  (Mier-Jedrzejowicz and Southwood, 1979; Lester *et al.*, 1983), 8 (Lester *et al.*, 1985) although Sutcliffe and Nielsen (1992) present events where it exceeds 10. The SABRE polarisation, derived from FFT and hodogram analysis, is linear in both cases at the latitude of the amplitude peak. Equatorward of the peak, the SABRE polarisation is ACW in agreement with the ACW polarisation observed on the ground at Nordli, which is also equatorward of the amplitude peak. Mier-Jedrzejowicz and Southwood (1979) found that ACW polarisation was associated with westward phase propagation of the Pi2 pulsation signals on the nightside.

#### 4.4 Discussion of case interval 3

The substorm interval from day 101, 1983, is characterised by a weak westward electrojet at the EISCAT cross but

westward velocities (eastward electrojet) at SABRE. Two Pi2 pulsations present in the magnetometer data have simultaneous signatures in the SABRE data. Initially, both SABRE and the Nordli magnetometer data appear to observe the same type of pulsation for the first event but the second observed by SABRE is totally different from that on the ground and seems to be driven by a separate source. The presence of a phase skip between the first and second pulsations seen simultaneously in both the ground magnetometer and SABRE data implies an impulsive source for this second pulsation (Mier-Jedrzejowicz and Hughes, 1980) with the driving function being switched on at the time of the phase skip. This second SABRE pulsation remains of the same large amplitude in both velocity components, is of longer period than on the ground, and, unlike the ground pulsation which decays, lasts for longer before stopping abruptly, perhaps when the source is switched off. There was also a phase skip apparent before the later pulsations that were not observed by SABRE. The high azimuthal wave number,  $m$ , suggested by the FFT analysis implies the presence of a fast mode wave in a relatively localised region of the ionosphere (Lester *et al.*, 1983).

McDiarmid and Allan (1990) modelled the coherent radar signature of a pulsation consisting of transient and cavity resonance driven components. This signature should include an amplitude envelope that is modulated with time and a pulsation period that changes during the course of the pulsation from two periods present at the start to only one towards the end. This occurs as the cavity resonance component period becomes dominant, the transient component having died-out. (Note that McDiarmid and Allan, 1990 do not comment on the ground magnetic signature of the wave.) In addition, there should be a latitudinal dependence of the pulsation period during the time of the transient pulsation, the longer field lines at higher latitudes producing a longer pulsation period. This should be apparent in the coherent radar Range-Time-Intensity (RTI) type data as a change in the slope of the on-off backscatter patch with latitude. When the slopes of the patches are all the same towards the end of the pulsation, the cavity resonance mode is dominant and the transient pulsation has died away. The study of such a pulsation was recently presented by McDiarmid *et al.* (1994). In the RTI from Wick for the interval on day 101, 1983 the patches of backscatter observed occur rather irregularly and over a limited latitude range, 66.0–67.6°N. The main poleward region of backscatter moves equatorward during the interval but there is no phase change with radar range apparent in the backscatter associated with the pulsation, i.e. there is no sloping of the backscatter patches observed.

The FFT-derived amplitude and phase analysis over the SABRE field of view at the dominant pulsation period suggested a fast mode compressional wave with  $m \sim 17$  and westward phase motion observed over the longitudinal extent of the field of view. The latitudinal phase variation was complicated at the position of the amplitude peak. The presence of the simultaneous phase skip poses the question of what switches on the second pulsation. Yeoman *et al.* (1992) observed storm-time Pc5 pulsations

with the Wick radar and these exhibited an  $m$  number similar to that recorded for the pulsation under investigation. In addition, the pulsations were strongly attenuated on the ground and had a period equal to the second or third harmonic of that in the Wick radar data. However, in the case of the storm-time Pc5s, the RTI from Wick did exhibit strong equatorward phase propagation with radar range so that they must be a different wave mode to that observed here. Yeoman *et al.* (1992) suggested that these Pc5 pulsations may be driven by wave-particle interactions. That would not seem to be the case for this study.

Further insight may be gained by considering the two separate signatures observed simultaneously by SABRE in time series data from different latitudes. The signature poleward of the FFT-derived amplitude peak in the SABRE field of view produces the ‘bay-like’ signature in the SABRE data, while the pulsation electric field produces an oscillatory signature equatorward of the amplitude peak. The dual source model for Pi2 pulsations (Yeoman *et al.*, 1990), includes an auroral zone impulsive source and a lower latitude cavity resonance driven source. The modelling of the signatures expected in coherent radar data by McDiarmid and Allan (1990) suggests the simultaneous and spatially coincident presence of two waves initially before the impulsive transient wave dies out and the cavity resonance driven wave becomes dominant. This was not apparent in the SABRE data.

A final possibility is that the two signatures which arise in the SABRE data at different latitudes result from a compressional surge of plasma earthward at substorm onset to produce the poleward ‘bay’ signature in the ionosphere which then couples to the density gradient at the plasmopause and produces a field line resonance. This then produces the transient oscillatory signature observed by SABRE at lower latitudes in the field of view. It is not certain how this fits in with the magnetometer signature of two temporally separate pulsations. Changing geophysical conditions e.g. the size of the magnetospheric cavity or a change in the plasma density, might explain the change in period of the waves observed on the ground. A different harmonic of the wave may be excited or the fast mode source may have coupled to a different field line. However, the appearance of a 90 s pulsation after a 60 s pulsation is harder to explain unless a different harmonic of the wave is excited on the geomagnetic field line.

Summarising this interval, the differences between the pulsation signatures observed by SABRE and on the ground by the magnetometer remain to be explained. The Nordli magnetometer is offset slightly in both latitude and longitude from the position in the SABRE field of view displaying the pulsation signatures so that some alteration to the signal may have taken place in travelling to the ground. The high  $m$  number recorded for the SABRE pulsation indicates a fairly localised event so that the Nordli magnetometer might not be close enough to observe the same pulsation signature. The ground pulsation signature is affected by changes in conductivity and during a substorm the height-integrated Hall and Pedersen conductances can change by an order of magnitude on time scales similar to the pulsation period. However, the different spectral characteristics but the same driving force

for the second pulsation suggest a more complicated coupling of wave modes, the exact nature of which remains unclear at the present time.

## 5 Summary and conclusions

Three case studies of substorm intervals containing Pi2 pulsations observed by SABRE under different prevailing magnetic conditions have been presented. The time series signature of the SABRE Pi2 pulsation is highly dependent on the position of the SABRE field of view relative to the substorm current wedge and/or pulsation generation region. This position obviously changes with local time and the level of magnetic activity, the auroral oval moves equatorwards and expands in width as activity increases. In two of the three case studies presented here, the SABRE field of view is situated either in the latitude/longitude sector where the ionospheric and FAC associated with the pulsation generation region move into and across the radar field of view or where the auroral zone signature of the pulsations changes to that observed at mid-latitudes. In the third interval, SABRE is equatorward of the substorm associated electrojets.

When magnetic activity is low, as in the third case study, the SABRE field of view is located equatorward of the auroral zone pulsation generation region. The signature in the SABRE time series is unexpectedly complex. The large pulsation amplitude in both components suggests the presence of two different wave modes. The results of SABRE FFT spectral analysis indicate that this signature results from a fast mode wave with high  $m$  number displaying westward phase propagation. The second pulsation during the low magnetic activity case study observed by SABRE and the ground magnetometers appears to be driven by the same impulsive source as a simultaneous phase skip is observed by the two instruments. There is however, little decay in amplitude in the SABRE signature before the wave ends abruptly. The exact nature of the driving mechanism for the second pulsation and the coupling involved between the complex ionospheric and classical, damped ground pulsation signatures remains unclear at present.

At times of higher magnetic activity the ionospheric and FAC associated with the substorm current wedge can be observed to move into the SABRE field of view. In the first case study, the substorm current wedge currents move westwards across the longitudes of SABRE field of view and the polarisation and spectral characteristics of the two Pi2 pulsations observed by SABRE at this time could be explained by these changes. During the second case study, the currents move equatorward into the field of view and then poleward out of it over the course of four Pi2 pulsations. Again the observations delimited two separate regions associated with the spectral content of the four Pi2 pulsations observed. A field line resonance generation mechanism may be able to account for these spectral differences.

In all three case studies there is evidence to support a twin source model of Pi2 pulsation generation (Yeoman *et al.*, 1990). In the first case study, two regions of opposite

polarisation sense were observed separated in latitude and longitude which may be indicative of the twin travelling wave source suggested in the model. The second case study contained pulsations in SABRE from the auroral zone pulsation generation region. These pulsations had periods greater than the corresponding period from the Wick ground magnetometer station at lower latitude. At the time of the final pulsation in the series SABRE observed two pulsation signatures separated in both latitude and longitude. In the lower latitude region of the field of view, the pulsation had a period roughly equal to that observed by the ground magnetometer at Wick. At the highest latitudes in the field of view, a pulsation of longer period was observed associated with a region of poleward velocity. As the EISCAT cross magnetometer data indicate that the substorm enhanced electrojets and FAC had moved poleward prior to the final pulsation, the longer period pulsation is associated with the auroral zone source while the shorter period pulsation is associated with a lower latitude source. During the third case study, SABRE observed a separate and distinct signature poleward of an oscillatory pulsation signature. The pulsation signatures observed were different in the SABRE and ground magnetometer data. Both the magnetometer and SABRE data contained two pulsations during the interval although they displayed different signatures for the second pulsation. The exact relationship between the driven ionospheric and classical, damped ground pulsation signatures observed is unclear at present as is the nature of the driving mechanism.

*Acknowledgements.* SABRE was a joint project between the University of Leicester, the Max Planck Institut für Aeronomie, Lindau, and the Swedish Institut för Space Physics, Uppsala. The BGS magnetometer network was deployed and maintained by the Geomagnetism Research Group of the British Geological Survey in Edinburgh. EGB acknowledges the receipt of a SERC CASE award with the BGS in Edinburgh and also support from SERC research grant GRH32025. Magnetometer Data from the EISCAT cross array were provided for the intervals of interest to this investigation by H. Lühr, University of Braunschweig. The authors would like to thank the referees for their constructive comments.

The Editor in Chief thanks D. Orr and another referee for their help in evaluating this paper.

## References

- Baumjohann, W., R. J. Pellinen, H. J. Opgenoorth, and E. Nielsen, Joint two-dimensional observations of ground magnetic and electric fields associated with auroral zone currents 4. Current systems associated with local auroral break-ups, *Planet. Space Sci.*, **29**, 431–447, 1981.
- Björnsson, A., O. Hillebrand, and H. Voelker, First observational results of geomagnetic Pi2 and Pc5 pulsations on a north-south profile through Europe, *Z. Geophys.*, **37**, 1031–1042, 1971.
- Bradshaw, E. G., SABRE and magnetometer studies of substorm associated pulsations, Ph.D. Thesis, University of Leicester, Leicester, UK, 1989.
- Bradshaw, E. G., M. Lester, and T. B. Jones, SABRE observations of structured ionospheric flows during substorm expansion phase onset, *Ann. Geophysicae*, **12**, 1027–1038, 1994.
- Chen, L., and A. Hasegawa, A theory of long period magnetic pulsations. 1. Steady state excitation of a field line resonance, *J. Geophys. Res.*, **79**, 1024–1032, 1974.
- Fukinishi, H., Polarisation changes of geomagnetic Pi2 pulsations associated with the plasmopause, *J. Geophys. Res.*, **80**, 98–110, 1975.
- Gelpi, C., W. J. Hughes, H. J. Singer, and M. Lester, Mid-latitude Pi2 polarisation pattern and synchronous orbit magnetic activity, *J. Geophys. Res.*, **90**, 6451–6458, 1985.
- Hughes, W. J., The effect of the atmosphere and ionosphere on long period magnetospheric micropulsations, *Planet. Space Sci.*, **22**, 1157–1172, 1974.
- Kisabeth, J. L., and G. Rostoker, Current flow in auroral loops and surges inferred from ground-based magnetic observations, *J. Geophys. Res.*, **78**, 5573–5584, 1973.
- Lester, M., W. J. Hughes, and H. J. Singer, Polarisation patterns of Pi2 magnetic pulsations and the substorm current wedge, *J. Geophys. Res.*, **88**, 7958–7966, 1983.
- Lester, M., W. J. Hughes, and H. J. Singer, Longitudinal structure in Pi2 pulsations and the substorm current wedge, *J. Geophys. Res.*, **89**, 5489–5494, 1984.
- Lester, M., K.-H. Glassmeier, and J. Behrens, Pi2 pulsations and the eastward electrojet: a case study, *Planet. Space Sci.*, **33**, 351–364, 1985.
- Lester, M., H. J. Singer, D. P. Smits, and W. J. Hughes, Pi2 pulsations and the substorm current wedge: low-latitude polarization, *J. Geophys. Res.*, **94**, 17133–17141, 1989.
- Lühr, H., S. Thürey, and N. Klöcker, The EISCAT magnetometer cross. Operational aspects – first results, *Geophys. Surveys*, **6**, 305–3, 1984.
- McDiarmid, D. R., and W. Allan, Simulation and analysis of auroral radar signatures generated by a magnetosphere cavity mode, *J. Geophys. Res.*, **95**, 20,911–20,922, 1990.
- McDiarmid, D. R., T. K. Yeoman, I. F. Grant, and W. Allan, Simultaneous observations of a travelling vortex structure in the morning sector and a field line resonance in the postnoon sector, *J. Geophys. Res.*, **99**, 8891–8904, 1994.
- McPherron, R. L., C. T. Russell, and M. P. Aubry, Satellite studies of magnetospheric substorms on August 15, 1968. 9. Phenomenological model for substorms, *J. Geophys. Res.*, **78**, 3131–3149, 1973.
- Mier-Jedrzejowicz, W. A. C., and D. J. Southwood, The east-west structure of mid-latitude geomagnetic pulsations in the 8–25 mHz band, *Planet. Space Sci.*, **27**, 617–630, 1979.
- Mier-Jedrzejowicz, W. A. C., and W. J. Hughes, Phase skipping and packet structure in geomagnetic pulsation signals, *J. Geophys. Res.*, **85**, 6888–6892, 1980.
- Nielsen, E., W. Guttler, E. C. Thomas, C. P. Stewart, T. B. Jones, and A. Hedberg, SABRE – a new radar auroral backscatter experiment, *Nature*, **304**, 712–714, 1983.
- Pashin, A. B., K.-H. Glassmeier, W. Baumjohann, O. M. Raspopov, A. G. Yahnin, H. J. Opgenoorth, and R. J. Pellinen, Pi2 magnetic pulsations, auroral break-ups and the substorm current wedge: a case study, *J. Geophys. Res.*, **51**, 223–233, 1982.
- Rostoker, G., The polarization characteristics of Pi2 micropulsations and their relation to the determination of possible source mechanisms for the production of night-time impulsive micropulsation activity, *Can. J. Phys.*, **45**, 1319–1335, 1967.
- Samson, J. C., and B. G. Harrold, Maps of the polarisation of high latitude Pi2's, *J. Geophys. Res.*, **88**, 5736–5744, 1983.
- Samson, J. C., and G. Rostoker, Polarisation characteristics of Pi2 pulsations and implications for their source mechanism; influence of the westward travelling surge, *Planet. Space Sci.*, **31**, 435–458, 1983.
- Sergeev, V. A., L. I. Vagina, R. D. Elphinstone, J. S. Murphree, D. J. Hearn, L. L. Cogger, and M. L. Johnson, Comparison of UV spectral signatures with the substorm current wedge as predicted by an inversion algorithm, *J. Geophys. Res.*, **101**, 2615–2627, 1996.
- Southwood, D. J., Some features of field line resonances in the magnetosphere, *Planet. Space Sci.*, **22**, 483–491, 1974.
- Southwood, D. J., and W. F. Stuart, 'Pulsations at the substorm onset', in *Dynamics of the Magnetosphere* (Ed. S.-I. Akasofu, D. Reidel, Dordrecht, Netherlands, 1980).

- Southwood, D. J., and W. J. Hughes**, Theory of hydromagnetic waves in the magnetosphere, *Space Sci. Rev.*, **35**, 301–366, 1983.
- Southwood, D. J., and W. J. Hughes**, Concerning the structure of Pi2 pulsations, *J. Geophys. Res.*, **90**, 386–392, 1985.
- Stuart, W. F.**, A special feature of impulsive pulsations (Pi2), *J. Atmos. Terr. Phys.*, **34**, 829–8, 1972.
- Sutcliffe, P. R., and E. Nielsen**, STARE observations of Pi2 pulsations, *Geophys. Res. Lett.*, **17**, 603–606, 1990.
- Sutcliffe, P. R., and E. Nielsen**, The ionospheric signature of Pi2 pulsations observed by STARE, *J. Geophys. Res.*, **97**, 10621–10636, 1992.
- Waldock, J. A., D. J. Southwood, M. P. Freeman, and M. Lester**, Pulsations observed during high-speed flow in the ionosphere, *J. Geophys. Res.*, **93**, 12883–12891, 1988.
- Yeoman, T. K., and D. Orr**, Phase and spectral power of mid-latitude Pi2 pulsations: evidence for a plasmaspheric cavity resonance, *Planet. Space Sci.*, **37**, 1367–1383, 1989.
- Yeoman, T. K., D. K. Milling, and D. Orr**, Pi2 polarisation patterns on the UK Sub-Auroral Magnetometer Network (SAMNET), *Planet. Space Sci.*, **38**, 589–602, 1990.
- Yeoman, T. K., M. Lester, D. K. Milling, and D. Orr**, Polarisation, propagation and MHD wave modes of Pi2 pulsations: SABRE/SAMNET results, *Planet. Space Sci.*, **39**, 983–998, 1991.
- Yeoman, T. K., Mao Tian, M. Lester, and T. B. Jones**, A study of Pc5 hydromagnetic waves with equatorward phase propagation, *Planet. Space Sci.*, **40**, 797–810, 1992.